

NUCLEAR
INSTRUMENTS
& METHODS
IN PHYSICS
RESEARCH
Section A

Ultrafast Waveguiding Quantum Dot Scintillation Detector

K. Dropiewski^a, A. Minns^a, M. Yakimov^a, V. Tokranov^a, P. Murat^b, and S. Oktyabrsky^{a*}

^aSUNY Polytechnic Institute, 257 Fuller Rd, Albany 12203, USA

^bFermi National Accelerator Labratory , PO Box 500, Batavia 60510, USA

Elsevier use only: Received date here; revised date here; accepted date here

Abstract

Picosecond timing of energetic charged particles and photons is a challenge for many high-energy physics and medical applications. InAs Quantum Dots (QDs) embedded in GaAs matrix are expected to have unique scintillation properties. The advantages come from highly efficient energy conversion as well as from fast electron capture and radiative recombination in QDs. We present design considerations and demonstration of an ultrafast, high photon yield room-temperature semiconductor scintillator. Due to high refractive index of the semiconductor, the scintillator is fabricated in the form of 20 μm thick planar waveguide with an integrated InGaAs photodiode. QD luminescence have shown about 50% efficiency at room temperature and modal attenuation stabilized at 1 cm⁻¹. Scintillation response from 5.5 MeV alpha-particle shows extremely fast decay time of 280 ps, 11% collection efficiency and time resolution of 60 ps. The data confirm unique potential properties of this scintillation detector.

© 2001 Elsevier Science. All rights reserved

Keywords: Scintillation Detector, Scintillator, Quantum Dot, GaAs, InAs, Molecular Beam Epitaxy

^{*}Corresponding author. Tel.: +1-518-437-8688; e-mail: soktyabrsky@sunypoly.edu.

1

2

3

4

6 7

8

9

10

11

12

13 14

15

16

43

44

45

46

1. Introduction

Picosecond range time resolution for scintillation detectors, is currently highly sought after yet largely unobtained, particularly in the fields of high-energy physics and medical imaging. While significant improvements have been to incorporate time-of-flight capability into PET scanners [1, 2], inorganic scintillators operate close to their physical resolution limit due to relatively long rise and decay times and insufficient light yield. [3-6]. Therefore fast scintillation detectors remain an obstacle for, high-energy physics and calorimetry, which critically need better timing resolution, for example, for subatomic particle observations [7] and for medical applications where precise time-of-flight information reduces patient exposure to ionizing radiation [8]. For these applications, direct band gap semiconductor scintillation materials have been largely ignored because of their physical limitations, such as slow luminescence and high self-absorption, low material density/stopping power that make them too slow. Their high self-absorption compared to inorganic scintillators meant that they relied on multiple absorption and re-emission events, while their low stopping power necessitated thick scintillators in the direction of incidence. Comparatively, InAs quantum dots (QDs) functioning as luminescence centers embedded in a GaAs matrix can have uniquely fast scintillation properties with low selfabsorption [9]. The advantage comes from high efficiency radiation energy conversion, as well as the fast electron capture in this high-mobility material and fast radiative recombination in the strongly localized potential of QDs.

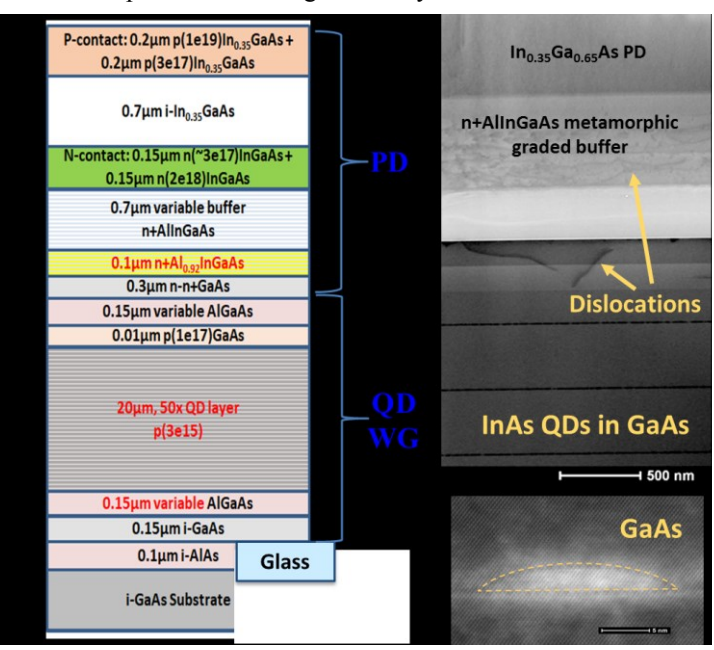


Figure 1. (a) Layout of the heterostructure with a PD and QD/WG matrix as grown by MBE, showing the position of foreign substrates such as glass after layer transfer. (b) STEM BF cross-sectional image of top of the 20 μ m thick waveguide and bottom of the photodiode section. (c) STEM HAADF cross-sectional image of an individual QD: InAs contrast appears as bright. Outline of QD shown as dotted line. QD density is $\sim 5 \times 10^{10}$ cm⁻² and average lateral size is 14nm.Color online.

We present a design and major considerations for demonstration of an ultrafast, high photon yield roomtemperature semiconductor scintillator based on InAs ODs embedded in a GaAs matrix. The detector consists of three integrated physical systems. First, GaAs, the radiation stopping material, is a direct band gap semiconductor resulting in high photon yield (~240,000 photons/MeV). GaAs also has high electron mobility resulting in fast electron transport to the QDs and capture $\sim 2-5$ ps [10, 11]. Embedded InAs QDs are red-shifted >300 mV from the bandgap of GaAs matrix, resulting in low self-absorption (~1 cm⁻¹). Previously, fast luminescence decay time was documented for InAs QDs (~0.5-1 ns) [11, 12].

Second, the GaAs matrix due to its high refractive index acts as a waveguide (WG) for QD luminescence to provide efficient light collection. For the proposed scintillator, only ~2% of randomly emitted photons are transmitted through a

planar interface with air. Therefore, a favorable solution is to extract light from the waveguide with an integrated photodetector (PD) comprising the third system, Then the waveguiding can provide the coupling efficiency between scintillator and PD close to 100%.

2. Methods

The structure shown in Fig. 1 was deposited using molecular beam epitaxy (MBE) in an EPI Mod Gen II system. A 100 nm thick AlAs sacrificial layer was grown on the GaAs substrate to further separate the QD WG layer and transfer it to a foreign substrate such as glass slide using epitaxial lift-off [13]. The bottom of the waveguide is a 150 nm variable $Al_{0.3-0.1}Ga_{0.7-0.9}As$ barrier layer to reduce surface recombination of photocarriers. The QD scintillator/WG matrix is composed of a 20 μ m GaAs layer grown at 590 0 C with 50 embedded sheets of InAs QDs. Each QD sheet is prepared as ~2 ML thick self-assembled InAs at 520 0 C, capped with ~2 ML of AlAs to control the shape of the QDs and improve uniformity as shown in Ref. [14, 15]. The intermediate GaAs layers are modulation p-type doped to facilitate fast capture of electrons. To cap the QD scintillator/WG matrix another 150 nm thick variable $Al_{0.3-0.1}Ga_{0.7-0.9}As$ layer is grown on top.

An integrated scintillation detector contains the QD/WG and a photodetector (PD as labeled in Fig. 1a) tuned to the QD emission wavelength. The photodiode is composed of a n^+ -type contact of 300 nm $In_{0.35}Ga_{0.65}As$, a 700 nm $In_{0.35}Ga_{0.65}As$ absorber and a p^+ -type contact of 400 nm $In_{0.35}Ga_{0.65}As$, all grown at 450 ^{0}C This structure also contains a metamorphic graded buffer layer between the QD/WG and the PD containing 700 nm of $Al_{0.92-0.6}In_{0.03-0.35}Ga_{0.05}As$ grown at 350 ^{0}C , intended to relieve strain (Fig. 1b). The low-Indium high-Al portion of the buffer is oxidized during TEM specimen preparation, but the upper portion shows the relaxed metamorphic layer confining most of the misfit dislocation, and preventing dislocation threading into the absorber (Fig. 1b).

The PD is fabricated using two lithography masks process with forming of the photodetector mesa and metallization of the PD contacts. After these processing steps, the majority of the structure is a QD/WG with a small area PD on the top surface. Finally, a QD waveguides with fabricated PDs were separated from GaAs substrate using epitaxial lift-off and transferred to glass to evaluate timing and energetic characteristics using 5.5 MeV alpha particles from ²⁴¹Am as an excitation source. The source was collimated using an acrylic shield with an aperture 1.3 mm in diameter.

3. Results and Discussion

3.1. Temperature-dependent Photoluminescence

Fig. 2(a) presents photoluminescence (PL) spectra of a QD/WG samples as-grown on a GaAs substrate, taken from 77K to 450K. The excitation source was an unfocused red (630 nm) laser providing ~0.5W/cm² intensity on the sample, and PL was collected from the top surface. Figs. 2(a,b) show that PL efficiency drops fast at higher temperatures and saturates at low temperatures. This behavior is typically observed in QD structures and is mostly related to thermal escape of carriers from QDs at higher temperatures, while the internal luminescence

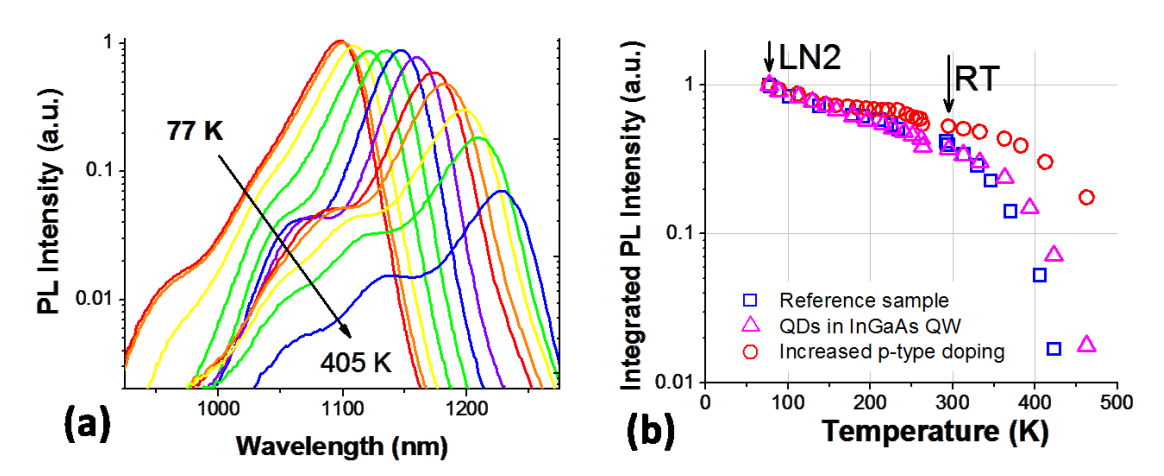


Figure 2. (a) Photoluminescence spectra of QDs taken from an as-grown structure from 77 K to 405 K. The spectra red-shift with increase of temperature due to bandgap reduction. (b) Integrated PL intensity as a function of temperature of InAs QDs with different shaping layer design and increased p-type modulation doping. Color online.

efficiency is approaching unity at low temperatures due to very fast capture and strong localization of photocarriers in the QDs [16]. In the present case, it can be assumed that the internal PL efficiency is close to unity at 77 K and is reduced to 40-60% at room temperature (RT).

Fig. 2(b) shows thermal quenching of integrated PL intensity of three samples with different QD engineering layers. The reference QD sample contained 2ML AlAs capping layers to increase the barriers for thermal escape of the carriers [14, 15]. In the second sample, similar QDs were placed into InGaAs quantum well to increase the capture rate into the dots. The third sample was engineered with 1.5x higher p-type modulation doing [12] than the reference sample, which contained 10 nm carbon-doped 1×10^{17} cm⁻³ layers centered between QD sheets that approximately provides 2 holes per dot. The sample with increased doping had three equidistant 5 nm thick layers with 1.5×10^{17} C/cm³ between the QD sheets corresponding to 3 holes per dot. The increased p-type doping resulted in an extraordinary high 60% efficiency at room temperature and 20% efficiency at 180 0 C.

3.2. Waveguide Attenuation

Fig 3(a) shows an experimental setup used to analyze attenuation in the QD/WG after complete etching off of the PD layers from the waveguide and transferring it to a glass substrate. The resulting 8.2 by 1.6 mm waveguide was excited by a 50 mW red (630 nm) laser, focused to a diameter $< 50 \mu m$ on the top surface. Light collection was via a multimode optical fiber coupled to the edge of the QD/WG. As the laser excitation point is moved away from the collection fiber (increasing x), PL spectra were collected at regular intervals (e.g. every $100 \mu m$).

There is a distinct red-shift of the spectra due to self-absorption in the QDs (Fig. 3b). Integrated PL intensity is shown in Fig. 3(c), in which the measurements were done with the collection fiber placed on the opposite sides of the sample. The initial high attenuation (as shown in the circle on the graph and image) represents a region in which PL collection efficiency falls due to initial drop of coupling between the waveguide and the fiber when the waveguiding (total internal reflection) is established. It is also affected by two-dimensional nature of waveguiding as it has a large width as compared to the collection fiber. Therefore, within the first \sim 1.5 mm of the sample the collection efficiency reduces with distance [9]. The spectrum at 1.5 mm (length = width) is shown with red circles in the Fig. 3(b) for reference.

After accounting these non-material sources of attenuation, the drop of luminescence intensity at shorter

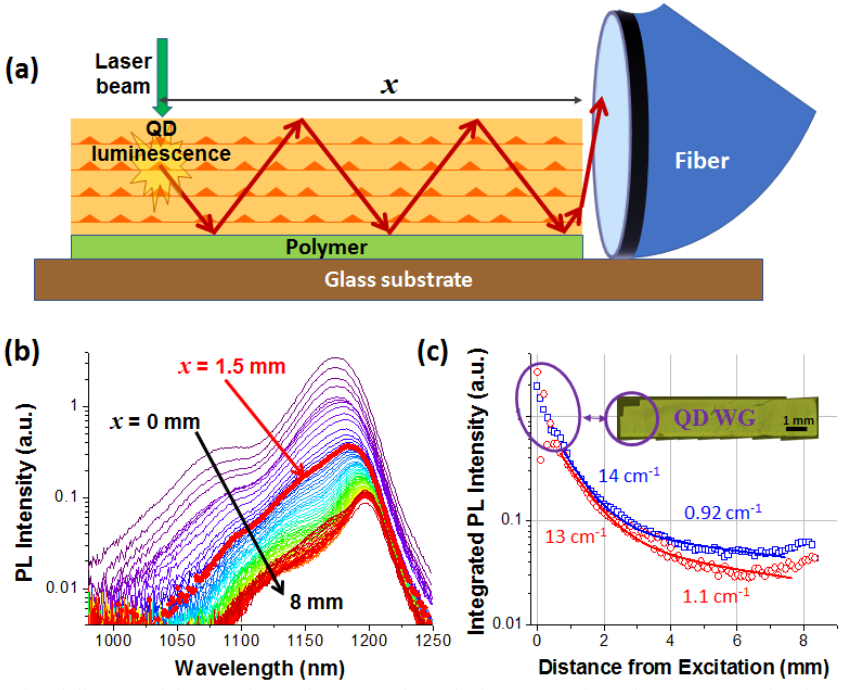


Figure 3. (a) Cross-sectional diagram of the experimental setup used to calculate attenuation. (b) PL spectra taken by a multi-mode fiber from the edge of the waveguide while scanning the laser excitation spot over the QD waveguide. Spectrum at x=1.5mm is shown by red dots. (c) Integrated PL intensity as a function of laser excitation spot distance from the collection fiber. Circles (red) had fiber positioned on side of WG with circle, squares (blue) were taken with fiber positioned on opposite side. Color online.

wavelengths (1050-1150 nm in this sample) occurs with \sim 14 cm⁻¹ level where mostly the luminescence from QD excited states is absorbed. The excited state QD emission is a manifestation of high laser excitation when more than two electrons occupy a single QD [17]. This is typically a rare case for the scintillation processes and we expect that it will be less significant for the scintillation detector applications. At longer distances (x > 3mm), the attenuation stabilizes at low level of \sim 1 cm⁻¹, which corresponds to \sim 0.5 cm⁻¹ of material absorption if multimode transmission is considered.

It is important to note that for this structure with 1.3×10^{15} cm⁻³ volume QD density this absorption coefficient is over 2 orders of magnitude less than that at the semiconductor band-edge (870 nm for GaAs). This reduced self-absorption resembles that of an "ideal" scintillator based, for example, on co-doped CdS(Te,In) to produce deep luminescent centers [18]. QD electronic structure plays a role of a deep center with high luminescence efficiency, fast capture and low controlled density.

3.3. Alpha Particle Response

Fig. 4 shows the results collected from a QD/WG with integrated PD using ²⁴¹Am 5.5 MeV alpha particles as an excitation source. Fig. 4 (a) shows alpha particle responses, collected at a rate of about 50 pulses per minute. The QD medium exhibited very fast luminescence decay of 280 ps at room temperature [19-21]. This waveguide structure allowed for collection on average 11% of the maximum of 5.5MeV photoexcited charge

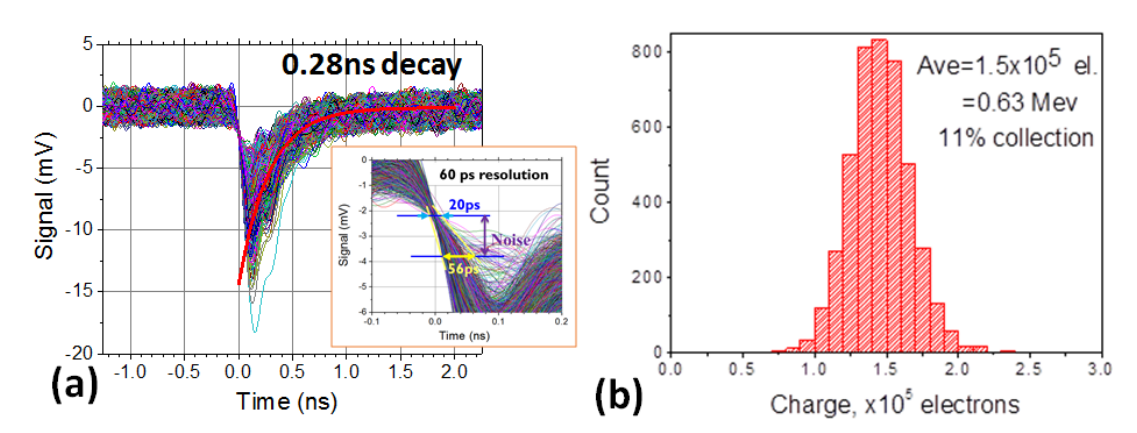


Figure 1. (a) Alpha-particle detection by integrated scintillation detector as in Fig. 1. Inset is a close-up of the leading edge of the pulses with estimated jitter of \sim 60ps. (b) Histogram of charge collected from alpha particles on the photodiode with an average of 11% collection out of total 5.5 MeV of initial energy. Recorded pulses showing \sim 100 ps risetime and 280 ps decay time, and average collected charge corresponding to 0.63 MeV deposited energy. Color online.

(Fig. 4b). This can be estimated as 30,000 photoelectrons per 1MeV of incident energy given about 1MeV alpha-particle energy loss in air. These are extremely promising parameters for the detector geometry non-optimized yet for efficient photon collection. The timing pulse profile allows for evaluating of 60 ps noise-limited time resolution (inset in Fig. 4).

4. Conclusions

We have presented results on temperature-dependent PL, waveguide attenuation and alpha particle response of a promising new semiconductor scintillation detector consisting of epitaxial InAs quantum dots (QDs) in a GaAs semiconductor matrix. QD photoluminescence (PL) have shown about 50% efficiency at RT and 20% efficiency at 180 °C, encouraging results for a room temperature scintillation detector. Attenuation of QD PL in the GaAs waveguiding matrix shows some self-absorption, which stabilizes to a material absorption coefficient of 0.5 cm⁻¹. Scintillation response of 5.5 Mev alpha-particles from our InAs QD/WG with integrated PD shows the extremely fast decay constant 280 ps, 11% collection efficiency and time resolution of 60 ps. The data confirm unique potential properties of this scintillation detector.

134

139

147

Acknowledgments

- The authors would like to acknowledge support from the National Science Foundation under award DMR-
- 136 1708637 and the U.S. Department of Energy, Office of Science under Award Number DE-SC0019031. One of
- the authors (KD) is grateful to John Sullivan fund for supporting the attendance of the 2018 Symposium on
- Radiation Measurements and Applications (SORMA XVII).

References

- 140 1. Kadrmas, D.J., et al., Impact of Time-of-Flight on PET Tumor Detection. J of Nucl Med, 2009. 50(8): p. 8.
- 141 2. Lecoq, P., Pushing the limits in Time-Of-Flight PET imaging. IEEE Trans Radiat Plasma Med Sci, 2017. 1(6): p. 473-485.
- 142 3. Derenzo, S.E., et al., *The quest for the ideal inorganic scintillator*. Nucl Instrum Methods Phys Res A, 2003. **505**: p. 6.
- 4. Doroud, K. and M. Williams, *A new approach for improved time and position measurements for TOF-PET: Time-stamping of the photo-electrons using analogue SiPMs.* Nucl Instrum Methods Phys Res A, 2017. **849**: p. 16-19.
- 5. Gundacker, S., et al., *Precise rise and decay time measurements of inorganic scintillators by means of X-ray and 511 keV excitation.*Nucl Instrum Methods Phys Res A, 2018. **891**: p. 42-52.
 - 6. Lecoq, P., Development of new scintillators for medical applications. Nucl Instrum Methods Phys Res A, 2016. 809: p. 130-139.
- 7. Ronzhin, A., et al., *Development of a 10ps level time of flight system in the Fermilab Test Beam Facility.* Nucl Instrum Methods Phys Res A, 2010. **623**(3): p. 931-941.
- 8. Conti, M., et al., Comparison of Fast Scintillators With TOF PET Potential. Nuclear Science, IEEE Trans Nucl Sci, 2009. **56**(3): p. 926-933.
- 9. Oktyabrsky, S., et al., *Integrated Semiconductor Quantum Dot Scintillation Detector: Ultimate Limit for Speed and Light Yield.* IEEE Trans Nucl Sci, 2016. **63**(2): p. 656-663.
- 15. Gündoğdu, K., et al., Ultrafast electron capture into p-modulation-doped quantum dots. Appl Phys Lett, 2004. 85(20): p. 4570-4572.
- 11. Zhang, L., et al., Dynamic response of 1.3-μm-wavelength InGaAs/GaAs quantum dots. Appl Phys Lett, 2000. 76(10): p. 1222-1224.
- 12. Bhattacharya, P., et al., *Carrier dynamics and high-speed modulation properties of tunnel injection InGaAs-GaAs quantum-dot lasers.*157 IEEE J Quantum Electron, 2003. **39**(8): p. 952-962.
- 13. Yablonovitch, E., et al., Extreme selectivity in the lift-off of epitaxial GaAs films. Appl Phys Lett, 1987. 51(26): p. 2222-2224.
- 14. Tokranov, V., et al., Shape Engineered InAs Quantum Dots with Stabilized Electronic Properties. Mat Res Soc Symp Proc, 2003. 737.
- 15. Tokranov, V., et al., *Enhanced thermal stability of laser diodes with shape-engineered quantum dot medium.* Appl Phys Lett, 2003. **83**(5): p. 833-835.
- 16. Oktyabrsky, S., et al., *Room-temperature defect tolerance of band-engineered InAs quantum dot heterostructures.* J Appl Phys, 2005. **98**(5): p. 053512.
- 17. Zhang, L., et al., *Excited-state dynamics and carrier capture in InGaAs/GaAs quantum dots.* Appl Phys Lett, 2001. **79**(20): p. 3320-3322.
- 18. Derenzo, S., et al., The quest for the ideal inorganic scintillator. Nucl Instrum Methods Phys Res A, 2003. 505(1): p. 111-117.
- 167 19. Oktyabrsky, S., et al. Nanoengineered quantum dot medium for space optoelectronic devices. in SPIE Optical Engineering+
 Applications. 2012: International Society for Optics and Photonics.
- 20. Yu, H., et al., Time resolved study of self-assembled InAs quantum dots. Appl Phys Lett, 1996. 69.
- 170 21. Yang, W., et al., *Effect of carrier emission and retrapping on luminescence time decays in InAs/GaAs quantum dots.* Phys Rev B, 1997. **56**.